GEOLOGICA CARPATHICA, 2025, 76, 3, 155–170 https://doi.org/10.31577/GeolCarp.2025.08

Cretaceous hydrothermal remobilization in the Central Western Carpathians: Dating of monazite-(Ce), xenotime-(Y), and hematite

JURAJ MAJZLAN[1,✉], PETR JEŘÁBEK[2], STEFAN KIEFER[1], MARTIN ŠTEVKO[3], MARTIN CHOVAN[4], JAROSLAV PRŠEK[5], KHULAN BERKH[6], PETER REINERS[7] and ISTVÁN DUNKL[8]

[1]Institute of Geosciences, Friedrich-Schiller University Jena, Germany
[2]Institute of Petrology and Structural Geology, Faculty of Science, Charles University, Prague, Czech Republic
[3]Institute of Earth Sciences, Slovak Academy of Sciences, Bratislava, Slovakia
[4]Department of Mineralogy, Petrology and Raw Materials, Comenius University, Bratislava, Slovakia
[5]Department of Economic Geology, AGH University of Kraków, Kraków, Poland
[6]Federal Institute of Geosciences and Raw Materials, Hannover, Germany
[7]Arizona Radiogenic Helium Dating Lab, University of Arizona, USA
[8]Department of Sedimentology and Environmental Geology, Georg-August-University Göttingen, Germany

(Manuscript received February 2, 2025; accepted in revised form July 2, 2025; Associate Editor: Milan Kohút)

Abstract: In this work, we investigated two regionally distributed and economically unimportant mineralizations. The first – quartz–hematite mineralization is found as veinlets and fracture filling, both in Variscan basement rocks and in Lower Triassic sandstones in the Tatric Unit. Using (U–Th)/He analysis, one hematite sample from Magurka–Kapustisko was dated to 97.5±4.4 Ma; another sample gave a lower precision age of 71±40 Ma. Previous geological and fluid-inclusion evidence suggests that the formation of the hematite veinlets could be linked to fluids expelled from the soles of moving thick- or thin-skinned nappes. The second studied mineralization consists of quartz with chlorite, tourmaline and REE phosphates monazite-(Ce) or xenotime-(Y), embedded in older mineralizations (siderite–ankerite veins – Čierny Balog, Jedľové Kostoľany, or metamorphosed hematite–magnetite ores – Bacúch). Our sample set was augmented by one metamorphic rock with REE phosphates (site Muráň; all samples from Veporic Unit). The U–Pb (LA-ICP-MS) ages from Jedľové Kostoľany, Čierny Balog and Muráň fall into a narrow range of 81–86 Ma, with one outlier at 77 Ma. The ages from Bacúch are somewhat older, between 87 and 92 Ma. The older ages from the nothernmost part of the Veporic unit reflect the progressive exhumation of this unit from north to south. At Jedľové Kostoľany, the ages of REE phosphates are only slightly older than those previously determined on hydrothermal muscovite, thus documenting lasting hydrothermal activity at these times. Large xenotime-(Y) crystals from Čučma (Gemeric Unit), associated with apatite, gave a spread of ages, with the main peak centered at 143±2 Ma. This age likely corresponds to Early Cretaceous compression, folding, and thrusting in the Gemeric Unit. An older event, located in our data at 183±3 Ma, corresponds to pre-existing, partially remobilized mineralization, recorded also in previously published ages related to uraninite. Remobilization was probably caused by unroofing of the Variscan basement of the Gemeric Unit and growth of the Meliata ocean basin.

Keywords: monazite, xenotime, hematite, radiometric dating, Central Western Carpathians, Alpine metamorphism, Alpine tectonics

Introduction

Western Carpathians (WC) are the northernmost segment of European Alpides (Schmid et al. 2008). They were formed by a number of Variscan and Alpine events of igneous, metamorphic, tectonic activity and sedimentary processes whose products modified or obliterated the pre-existing structures. The staggering complexity is an obstacle, but also an opportunity to link hydrothermal mineralizations to the orogenic events. The recognition of the sources of energy, fluids, and metals are simplified, to a certain small extent, by the large amount of geological and geochemical data accumulated over the last 150 years (see Grecula et al. 1995; Plašienka 2018; Kohút & Larionov 2021 for reviews on different aspects of the evolution of Western Carpathians).

Western Carpathians experienced the most vigorous phase of the Eoalpine orogenic activity in Cretaceous (Plašienka 2018). The trailing retrowedge (Inner WC) was inactivated already in the late Early Cretaceous whereas the leading prowedge (Outer WC) underwent modifications well into Cenozoic. The Central WC were shaped by the Cretaceous metamorphism (Jeřábek et al. 2008a; Faryad 1997), thrusting, burial, and exhumation (Lexa et al. 2003; Vojtko et al. 2016) that is recognizable in all of their major units. In all the resulting features, the approximately northvergent progression of the Eoalpine orogeny can be recognized.

✉ corresponding author: Juraj Majzlan
juraj.majzlan@uni-jena.de

The core of the Central WC is an agglomeration of thick-skinned crustal units. These are, from northwest to southeast, the Tatric, Veporic, and Gemeric units (Fig. 1). All these units contain Variscan basement rock with a variable degree of Variscan metamorphism and igneous activity (Bezák et al. 1993; Méres 2005; Putiš et al. 2009a; Faryad et al. 2020; Janák et al. 2020; Kohút & Larionov 2021; Spišiak et al. 2024). The Gemeric Unit experienced the episode of most important Eoalpine deformation and incorporation into the progressing orogen in Late Jurassic to Early Cretaceous (160–120 Ma) (Plašienka 2018). For the Tatric and Veporic units, the time of the most vigorous orogenic activity was Mid-Cretaceous (120–90 Ma). The degree of their Eoalpine metamorphic overprint is much different, though. The Veporic Unit underwent Eoalpine metamorphism up to conditions of amphibolite facies (Jeřábek et al. 2012) whereas the Tatric Unit experienced weak to none Alpine metamorphism (Plašienka 2018). All three units are covered by authochtonous sedimentary cover, generally of Permian–Mesozoic age. All of them were overridden by thin-skinned units, the Alpine nappes, designated as the Fatric, Hronic, and Silicic units (Fig. 1). Most commonly, the nappes are sequences of Mesozoic sedimentary rocks, occasionally with Permian strata or rarely with the underlying basement on their sole.

Large-scale orogenic activity was associated with fluid generation, circulation, and deposition of elements, thus, formation of hydrothermal mineralizations. They were divided into several stages in the Gemeric Unit (Hurai et al. 2008) and, for an easier comparison, these stages were correlated in terms of mineralogy to the mineralizations in Tatric and Veporic units (Majzlan et al. 2020a). Of relevance for this study are the siderite–ankerite, quartz–tourmaline, quartz–sulfide, and quartz–hematite stages (Hurai et al. 2008; Majzlan et al. 2020a), present in various proportions in the Veporic, Tatric, and Gemeric units.

Detailed knowledge of the tectonothermal evolution of the Western Carpathians, amassed over last decades, is an opportunity to link the ore mineralizations to that evolution. If successful, it may be easier to discern the sources of fluids, energy, and metals for these mineralizations. In this work, we investigated two regionally distributed uneconomic hydrothermal mineralizations in Central WC (CWC). Even though they were never subject of mining, they are interesting in terms of the metallogenesis of CWC. They are markers which help to constrain the age and formation of other types of mineralizations for which limited data exists. The principal method applied in this work is radiometric dating, supported by mineralogical description and chemical analyses of the minerals investigated. The samples come from occurrences whose mineralogy and geochemistry were investigated in detail in our previous work (Chovan et al. 1995; Pršek et al. 2010; Števko et al. 2014). In this work, therefore, we focus on the radiometric dating and the interpretation thereof.

One of the original goals of this work was to link the ages of the hydrothermal minerals to the vergency of the Alpine orogen. The working hypotheses, not fully confirmed by our work, was that the hydrothermal activity reached its peak during tectonic activation of the thick-skinned units and faded afterwards. This goal dictated the sampling pattern in the Tatric, Veporic, and Gemeric units. Samples were taken from ore bodies of different origin and from metamorphic rocks, focusing on minerals amenable to radiometric dating (monazite, xenotime, hematite).

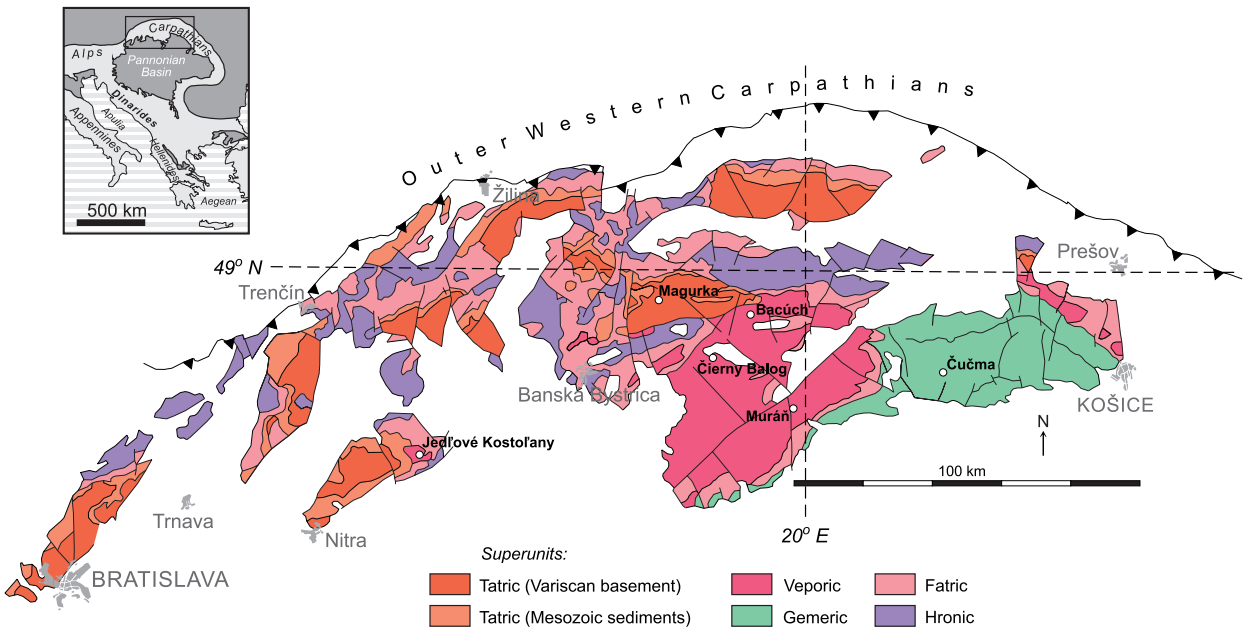

Fig. 1. Schematic geological map of the Central Western Carpathians (simplified after Lexa et al. 2000) with the position of major cities and the sampling sites. White areas are Neogene sedimentary and volcanic formations.

Ore mineralizations in the Central Western Carpathians

The siderite–ankerite stage is represented by large metasomatic or vein Fe deposits, especially in the Gemeric unit (Grecula et al. 1995), of great historical economic importance. The prime example thereof was the Droždiak vein in Rudňany, a large structure with length of 7 km, vertical extent 900 m, and thickness up to 40 meters filled by massive siderite, barite, and sulfides (Cambel et al. 1985; Grecula et al. 1995). A large deposit of metasomatic siderite in the Gemeric Unit was Nižná Slaná (e.g., Sasvári et al. 1996). Veins with similar mineral assemblages and their mutual temporal relationships occur also throughout the Tatric and Veporic units but are less common and much smaller there.

The quartz–tourmaline stage is in earlier Slovak literature referred to as the 'Alpine veins'. These are local, uneconomic veinlets or lenses with quartz, feldspars, chlorites, tourmalines, epidote, titanite, and REE phosphates, prominently developed especially in the Veporic and Gemeric units (Hurai et al. 1997). Monazite and xenotime, dated in this work from the localities Jedľové Kostoľany–Brezov štál, Bacúch–Biela Skala, Čierny Balog–Jergov, Čučma–Kutačka, is assumed to belong to the quartz–tourmaline stage.

In addition to the formation of veins with silicates and REE phosphates (the quartz–tourmaline stage or the 'Alpine veins'), older (Variscan or pre-Variscan) accessory minerals underwent also hydrothermal mobilization of some of their components (Ondrejka et al. 2022; Petrík et al. 2024). Monazite-(Ce) and xenotime-(Y) broke down to a new assemblage of fluorapatite and REE–B–Be silicates during Late Cretaceous retrograde metamorphism in the Veporic Unit. The sample from Muráň, used in this work, exemplifies such processes and complements the samples from the quartz–tourmaline veins.

The quartz–sulfide stage is commonly closely associated with the bodies of the siderite–ankerite stage. The association is spatial but there could be a genetic link as well, namely the ability of the carbonates to buffer pH and induce precipitation of the sulfide minerals. In some cases, the siderite–ankerite stage is prominent, in other cases, it may be subordinate, and quartz and sulfides occur with little or no carbonates (e.g., Luptáková et al. 2016). Breccia and cockade textures at some occurrences show siderite or ankerite fragments healed by quartz with sulfides (e.g., fig. 3e in Majzlan et al. 2020a). No textural evidence to the opposite was ever found and described, to our best knowledge.

The quartz–hematite stage was never of economic importance, being restricted to thin (a few cm) veinlets in crystalline basement or Lower Triassic sandstones. The veinlets are mostly found in the rocks of the Tatric Unit. Its importance lies in the fact that it appears to be the youngest hydrothermal stage, based on textural evidence (vein intersection) and on the fact that it penetrates into Triassic sedimentary rocks. Hence, knowing the age of this stage can constrain the age of the other hydrothermal stages as well. In this work, samples from Magurka–Kapustisko belong to the quartz–hematite stage.

Methods

Electron microprobe analyses

The measurement conditions of the wavelength-dispersive X-ray (WDX) analyses for the iron oxides were set to an accelerating voltage of 15 kV, a beam current of 15 nA, and a beam diameter of 1 μm. WDX was used to measure the following X-ray lines and elements: Kα of Al, Mg, Si, V, Cr, Ti, Fe, and Mn. The standards used for calibration were MgO for Mg, corundum for Al, wollastonite for Si, rhodonite for Mn, hematite for Fe, rutile for Ti, chromite for Cr, and a pure metal standard (100 %) for V.

The chemical composition of the REE phosphates was investigated for major and minor elements by electron microprobe analysis (EMPA) using a JEOL JXA-8230 at the University of Jena. The measurement conditions of wavelength-dispersive X-ray (WDX) analyses were set to an accelerating voltage of 20 kV, a beam current of 20 nA, and a beam diameter of 1 μm. WDX was used to measure the following X-ray lines and elements: Kα of Mg, F, Al, Na, Si, Cl, Mn, Ca, P, S, and Fe; Lα of As, Y, Nb, Dy, Ho, Tb, Er, Yb, Lu, Ba, Sr, La, Ce, Nd, Sm, Pr, Eu, Tm, and Gd; as well as Mα of Th, Pb, U, and Ta. The standards used for calibration were diopside for Mg, fluorite for F, InAs for As, corundum for Al, albite for Na, wollastonite for Si, Y–Al-garnet for Y, galena for Pb, halite for Cl, pure metal standards (100 %) for Nb and Ta, rhodonite for Mn, apatite for Ca and P, barite for Ba and S, celestine for Sr, hematite for Fe, and doped glass standards for Th, U, as well as Dy, Ho, Tb, Er, Yb, Lu, La, Ce, Nd, Sm, Pr, Eu, Tm, and Gd. Counting times were set to 100 s for U, Th, and the REE to improve count-rate statistics and 40 s the remaining elements. Overlap corrections were applied to avoid interference between the elements and lines of Er and Ho, Mn and Ba, Fe and Tb, Tm and Sm, Pb and Nb, Sr and Lu, Dy and Mn, Ho and Gd, Pr and La, Lu and Ho, Ta and Y, Mg and Eu, Tb and Ce, Tm and Sm, As and Mg, Al and Ho, Gd and Ce, Gd and La, Yb and Fe, Yb and Er, Dy and Eu, Tm and Ta, Eu and Pr, Eu and Dy as well as F and Ce. The detection limits were calculated from the background counts, the measurement time, and the standard material concentration, amount to 0.02 wt.% for Ho, Tb, Lu, Ca, La, Ce, Nd, Sm, Pr, and Eu; 0.03 wt.% for Cl, Dy, Er, Yb, Si, and Tm; 0.04 wt.% for Mn and Gd; 0.05 wt.% for Al, Si, Ba, and Mg; 0.06 wt.% for P and Fe; 0.07 wt.% for As, Th, Nb, Ta, Sr, and F; 0.08 wt.% for Na, Y, and U; as well as 0.09 wt.% for Pb.

Micro-X-ray fluorescence spectrometry

Element distribution maps of the cut samples were obtained using a μ-EDXRF M4 Tornado from Bruker Nano Analytics. A polychromatic excitation, emitted by a Rh tube, is focused through a polycapillary lens, resulting in a spot size of 17 μm (measured at Mo Kα). The emitted fluorescence from the sample is detected by two silicon drift detectors positioned opposite each other at 180°. This detector configuration is necessary

to eliminate diffraction signals that overlap with real element peaks in the spectrum. The X-ray tube was operated at 50 keV and 600 μA. Scanning was performed with a step size of 40 μm and a dwell time of 2 ms per pixel. Chemical compositions within selected regions of interest (ROIs) were calculated using mean spectra, applying the fundamental parameter method as implemented in the instrument's software.

Laser ablation ICP-MS analyses

The in-situ U–Pb dating of REE phosphates was performed by laser-ablation single-collector sector-field inductively coupled plasma mass spectrometry (LA-SF-ICP-MS) at Georg-August-University (Göttingen) and LASS-ICP-MS at the University of California (Santa Barbara, USA). The method employed for analysis in Göttingen is described in detail by Ring & Gerdes (2016) and Kohn & Vervoort (2008). A ThermoScientific Element 2 sector field ICP-MS was coupled to a RESOLution S-155 (Resonetics) 193 nm excimer laser (CompexPro 102) equipped with a two-volume ablation cell (Laurin Technic). All age data presented here were obtained by single spot analyses with a laser beam diameter of 15 μm and a crater depth of approximately 4 μm. The laser was fired at a repetition rate of 2 or 5 Hz, at nominal laser energy output of ca. 2 J/cm^2. Two laser pulses were used for pre-ablation. The carrier gas was He and Ar. Analytes of ^{238}U, ^{235}U, ^{232}Th, ^{208}Pb, ^{207}Pb, ^{206}Pb, mass 204, and ^{202}Hg were measured by the ICP-MS. The data reduction is based on the processing of ca. 46 selected time slices (corresponding ca. 13 seconds) starting ca. 3 sec. after the beginning of the signal. If the ablation hit zones or inclusions with highly variable actinide concentrations or isotope ratios then the integration interval was slightly resized or the analysis was discarded. The individual time slices were tested for possible outliers by an iterative Grubbs test (applied at P=5 % level). This test filtered out only the extremely biased time slices, and in this way usually less than 2 % of the time slices were rejected. The mass bias, inter-element fractionation, drift over the sequence time and the downhole fractionation were controlled and corrected by bracketing the unknown samples using NIST614 and 612 glasses and the GJ-1 zircon reference material (Jackson et al. 2004). The 44069 monazite reference material was used to correct the effect of the non- silicate matrix of the dated phases (Aleinikoff et al. 2006). The A49 (Vaaraslahti hypersthene granite), A276 (Viekkala gneiss), Weinsberg, and the 554 reference monazites were employed as "secondary age standards" and treated as unknowns during analysis (letter communication of D. Chew 2019; Friedl et al. 1996; Harrison et al. 1999, respectively). Drift- and fractionation corrections and data reductions were performed by our in-house software (UranOS; Dunkl et al. 2008). Data were plotted in the Tera-Wasserburg diagram and the ages were calculated as lower intercepts using Isoplot 3.75 (Ludwig 2012) and IsoplotR (Vermeesch 2018). All uncertainties are reported at the 2σ level.

The method employed for analysis in Santa Barbara is described in detail by Kylander-Clark et al. (2013). Analyses were carried out using a Photon Machines Excite 193 nm laser coupled to a Nu Instruments Plasma 3D (U–Pb isotopes) and an Agilent 7700 (element concentration), with an 8 μm spot at 3 Hz for 12 s, following a 2-pulse cleaning and 20 s baseline routine. Monazite reference material (RM) 44069 (424 Ma; Aleinikoff et al. 2006) was used as the primary U–Pb standard. Quality control was assessed by repeated measurements of Stern and FC-1 (512 and 55.6 Ma, respectively; Horstwood et al. 2003). The secondary RMs were within 1 % of their accepted values. Age uncertainties (2σ) expressed in the text correspond to analytical uncertainties. For each analysis, the ^{207}Pb/^{206}Pb- and ^{238}U/^{206}Pb-ratios were plotted on Tera-Wasserburg diagrams using the online version of IsoplotR (Vermeesch 2018). The space of concordant isotopic compositions is marked by the concordia line. For discordant U/Pb isotopic ratios we report an intercept age based on a Stacey-Kramers common-Pb value (Stacey & Kramers 1975).

(U–Th)/He dating

The U, Th, and He contents of selected hematite samples were measured following procedures outlined by Evenson et al. (2014) and Garcia et al. (2018) (University of Arizona). Aliquots for (U–Th)/He analysis were all fragments of larger polycrystalline aggregates ranging from 300 to 700 μm in length and 100 to 400 μm in length and width with masses <0.5 mg. Aliquots were separated with a steel needle. Magnetite admixture was removed by a magnet and pyrite/iron oxides were separated under binocular microscope. Aliquots weighing ~100–300 μm each were washed in pure water and then ethanol to remove detritus or contaminants, and weighed on a microbalance with precision of about 1 μm. Cleaned aliquots were then dried and packed into 1 mm Nb tubes and placed into a copper planchet. Aliquots were degassed by diode or CO_2 lasers in a high vacuum extraction line at temperatures ranging from approximately 1000–1200 °C for 12–18 min, and then re-extracted for an equally long or longer duration at a higher laser power and temperature. Re-extractions of helium yielded fractions less than 2–3 % of initial release in all cases. Two aliquots from each sample (Fe1 and Fe2 in Table 1) were lased at higher temperature

Table 1: Overview of the monazite-(Ce) and xenotime-(Y) U–Pb ages obtained on REE phosphates from this work and from literature. All localities are located in the Veporic unit.

locality	monazite-(Ce)	xenotime-(Y)
Bacúch	89.2±0.8	88.8±0.4
	91.6±0.9	89.4±0.5
	87.3±0.3	89.2±0.6
Jedľové Kostoľany	83±9 (Ozdín 2008)	81.8±1.0
		76.7±0.8
Čierny Balog		82.8±1.7
Muráň	83±0.5	
Heľpa	96±23 (Petrík et al. 2024)	
Ľubietová	92±11 and 97±9 Ma (Ozdín et al. 2016)	

(~1250 °C). Four aliquots from each sample were also analyzed for only U–Th concentrations, with no laser extraction for He, to check for U-loss by laser heating. With one exception (a single aliquot with extraordinarily high U content, Table 1), these undegassed aliquots showed similar U and Th concentrations as the degassed, dated aliquots, consistent with minimal U-loss during lasing (e.g., Hofmann et al. 2020). ^{4}He abundance of aliquots was measured relative to a ^{3}He spike by quadrupole mass spectrometry following Reiners (2005). Aliquots were dissolved and analyzed for U and Th concentrations by isotope dilution after the addition of a ^{233}U–^{229}Th spike on a ThermoFisher E2 ICP-MS.

Results

The location of all samples in Western Carpathians is shown in Fig. 1. The GPS coordinates for all sampled occurrences are listed in Suppl. Table S1.

Sample description

Hydrothermal quartz–tourmaline stage associated with siderite–sulfide veins

Samples from **Čierny Balog–Jergov** and **Jedľové Kostoľany–Brezov štál** represent veins of hydrothermal carbonates hosted by the rocks of the Veporic Unit. In Čierny Balog, the ore bodies are hosted by paragneisses with variable degree of retrograde metamorphic overprint. In Jedľové Kostoľany, the host rocks are gneisses and schists of the Tríbeč crystalline basement. The samples from Čierny Balog are coarse-grained (grain size up to 1 cm), beige carbonates with quartz lenses and veinlets (Fig. 2). Carbonates are heterogeneous, with evidence of multiple brecciation events, healing of the fractures, and overgrowth (Fig. 3). The earlier carbonates are Fe-richer than the later ones that contain more Mg and less Fe. Overall, most of the carbonates in these samples belong to magnesite (Mg>Fe on atomic basis). The earlier carbonates may also include grains of ankerite (white on Fig. 2) that are replaced and resorbed by the later Mg–Fe carbonates. The later carbonates may also include overgrowths or bands with higher Mn concentration (Fig. 3). All types of carbonates are cut by grains and veinlets of quartz and K-feldspars. The carbonates also contain small inclusions of REE phosphates and apatite. The EMP analyses confirmed the semiquantitative observations by μ-XRF in that the carbonates have more Mg than Fe (on molar basis; Suppl. Table S2, Fig. 4).

REE phosphates belong to xenotime-(Y) and form tiny anhedral grains, not larger than 10 μm, or aggregates of the grains up to 100 μm large. They are located in the carbonates and overprint the brecciation and healing features. These textures are interpreted as evidence of the younger age of xenotime-(Y) with respect to most or all carbonates in the samples.

The samples from Jedľové Kostoľany were coarse aggregates of brown, less commonly light gray carbonates with veinlets of quartz with chlorite. According to the μ-XRF scans, the light gray carbonates belong to the dolomite–ankerite series and appear to be older than the brown carbonates of the siderite–magnesite series (Fig. 5). Chalcopyrite is common and forms cluster up to 2 cm large. Microscopically, chalcopyrite is accompanied by euhedral pyrite crystals and thin veinlets of tetrahedrite. Lath-like muscovite crystals formed along the grain boundaries in siderite.

In siderite, brecciation and healing by younger carbonates is observed. The younger carbonates have slightly lower Fe/(Fe+Mg) values, i.e., are Mg-richer than the earlier

Fig. 2. Hand specimens from Čierny Balog, showing coarse-grained beige and white carbonates. From left to right: C3, C7, C8.

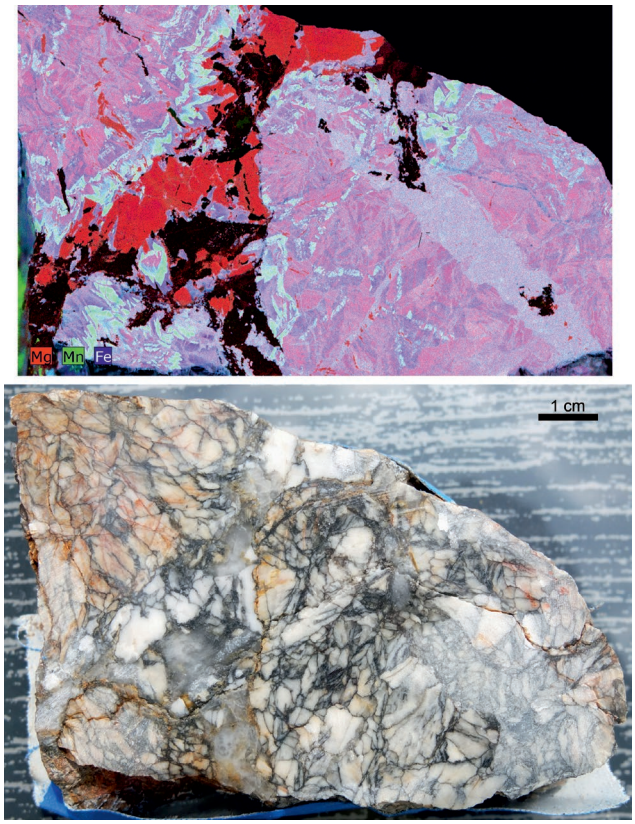

Fig. 3. Element distribution map (acquired by μ-XRF) for Mg, Mn, Fe in the sample C3 (Čierny Balog). The false colors in the upper panel for the elements shown were scaled to get the best contrast for the carbonate minerals and cannot be associated with any numerical values for the concentration of these elements. A macrophoto in the lower panel shows the analyzed sample. The sample consists essentially only of carbonates and quartz (shown here in black).

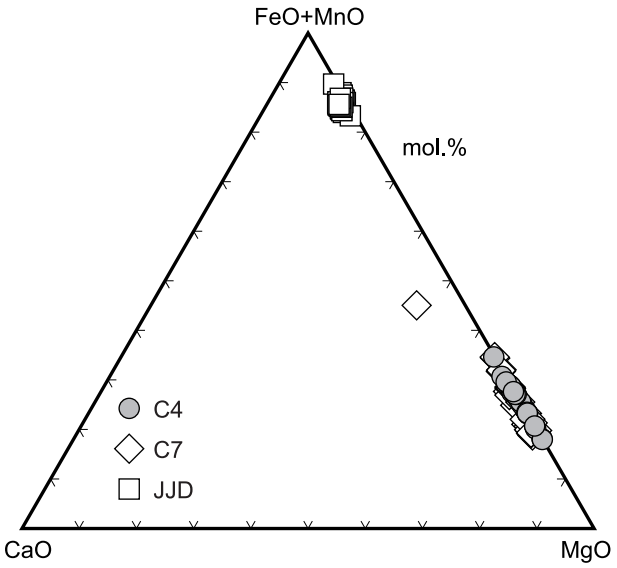

Fig. 4. Chemical analyses of hydrothermal carbonates from Čierny Balog (circles and diamonds) and Jedľové Kostoľany (squares). All data from electron microprobe.

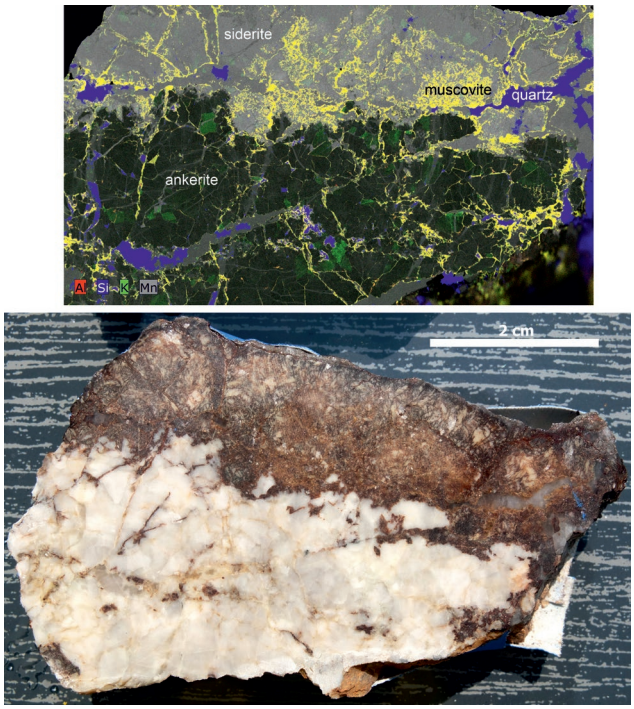

Fig. 5. Element distribution map (acquired by μ-XRF) for Al, Si, K, and Mn in the sample JJD3 (Jedľové Kostoľany). The false colors for the elements shown were scaled to get the best contrast for the carbonate minerals and cannot be associated with any numerical values for the concentration of these elements. A macrophoto in the lower panel shows the analyzed sample.

carbonates. The molar Fe/(Fe+Mg) ratio are high, almost 0.9, in all analyzed carbonates of the siderite–magnesite series (Fig. 4). REE phosphates belong to xenotime-(Y) and are tiny, not larger than 10 μm. They occur in carbonates but their temporal relationship to the carbonates is difficult to establish with certainty based on textural criteria.

The hydrothermal vein in **Čučma–Kutačka** contains U–REE mineralization. The vein consists mostly of quartz, with abundant and large (up to 3 cm) columnar fluorapatite crystals. REE phosphates are located between the apatite crystals or in the cracks in these crystals. They may be accompanied by uraninite or coffinite. Xenotime-(Y) forms banded, botryoidal aggregates. The overall thickness of these aggregates may reach 2 mm. For a detailed mineralogical and chemical description of the minerals in this assemblage, refer to Števko et al. (2014). They reported that rare florencite and goyazite are a part of the assemblage.

Xenotime-(Y) crystals from Čierny Balog, Jedľové Kostoľany, and Čučma were investigated with the electron microprobe. The normalized REE patterns for xenotime-(Y) from all three sites are shown in Suppl. Fig. S1. The REE inventory of xenotime-(Y) is dominated by middle and heavy REE's, dictated by crystal-chemical constraints of its structure. For the MREE, the differences can be seen especially for Eu, to a lesser extent also for Sm. The samples from Jedľové Kostoľany show a positive Eu anomaly, those from Čierny

Balog no anomaly, and the samples from Čučma a negative Eu anomaly. The differences in Sm content are also easily discernible. The highest Sm content was determined for the samples from Čierny Balog, followed by Čučma and Jedľové Kostoľany, with some overlap between the latter two. For the HREE, the most conspicuous variations are seen for Tm, with a number of samples from Čierny Balog showing anomalously low concentrations. The samples from Čučma contain in general more HREE's than the other samples.

The distribution of REE in the monazite-(Ce) crystals from Muráň was measured by LA-ICP-MS. The normalized distribution is shown in Suppl. Fig. S1. It shows monotonous decline from the light to the heavy REE, typical for monazite-(Ce). The data for the monazite-(Ce) from Bacúch show a similar trend, with greater scatter (lower precision) for the minor rare-earth elements.

Hydrothermal quartz–tourmaline stage in metamorphosed magnetite ores

The samples from **Bacúch–Biela Skala** are massive quartz–magnetite ores hosted by mica schists of the Veporic Unit. Bands of magnetite (Fig. 6) represent the primary sedimentary layering that was not obliterated by the Alpine metamorphism. Microscopic investigation confirmed quartz and magnetite as the dominant minerals. The quartz-rich bands contain a small amount of muscovite and chlorite. Magnetite is locally replaced by hematite. We note explicitly that this hematite does not belong to the quartz–hematite stage; hematite is a product of conversion from magnetite. Further mineralogical and geochemical details regarding these ores can be found in Pršek et al. (2010). They also reported the occurrence of accessory ilmenite, cassiterite, pyrite, galena, Bi sulfosalts, albite, K-feldspar, and tourmaline in these ores. Bulk of these ores is not of hydrothermal origin but they experienced hydrothermal overprint, resulting in formation or remobilization of some of the accessory minerals reported by Pršek et al. (2010), including the REE phosphates. The REE phosphates (monazite-(Ce) and xenotime-(Y)) form anhedral grains or aggregates up to 100 μm large. They are located in quartz and can be in contact with magnetite.

Metamorphic rocks of the Veporic Unit

The samples collected near Muráň (locality VV4) correspond to garnet-bearing micaschist of the Kohút zone in the Veporic superunit, located in the staurolite–biotite–kyanite zone 3 documented by Janák et al. (2001). The studied samples are composed of quartz, white mica, biotite, chlorite, rare plagioclase, garnet, and accessory rutile, ilmenite, and monazite-(Ce). The white mica is formed by intergrowths of muscovite and paragonite. Garnet grains (up to 4 mm large) are locally fractured and show replacement of the earlier garnets by younger grossular-rich overgrowths. The samples show two fabrics with domain appearance manifested by alternation of cleavage domains with the younger fabric and lithon domains with the older fabric. The cleavage is occupied by finer grained white mica matrix and lithons show folded coarser grained white mica and quartz bands. The studied monazite-(Ce) occurs in both finer grained and coarser grained white mica matrix.

Hydrothermal quartz–hematite stage

The samples from **Magurka–Kapustisko** are hematite–quartz veinlets in rocks of the Tatric Unit in the Nízke Tatry Mts. The veinlets are hosted by pegmatites of the Variscan porphyric granites of the Prašivá type and Lower Triassic sandstones. The veinlets are abundant but only a few millimeters thick. The most common mineral is hematite; quartz

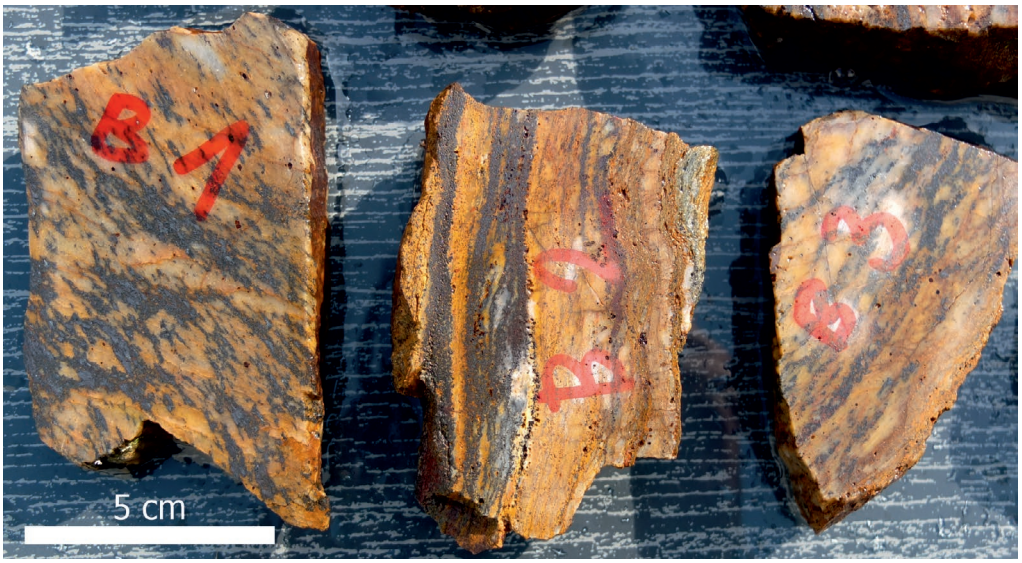

Fig. 6. Hand specimens from Bacúch, showing the magnetite bands in quartz.

crystals can be found in small cavities. In some cases, hematite is accompanied by powdery, secondary iron oxides that are assumed to be a weathering product of pyrite. Microscopic investigation revealed the presence of magnetite that is replacing the hematite crystals (Fig. 7). Furthermore, both hematite and the pseudomorphs of magnetite show porosity that seems to postdate the formation of both minerals. In one of the samples, a few tiny (<2 μm) grains with Cu and Zn were detected by EDX analyses. Further details on the mineral and chemical composition of the ore veins at Magurka were given by Chovan et al. (1995).

Hematite and magnetite are chemically almost pure (for electron-microprobe analyses of hematite, see Suppl. Table S3). The only metal (apart from Fe) that is consistently above the detection limit of the electron microprobe is Ti, with up to 0.6 wt.% TiO_2 in hematite in the sandstones and up to 1.3 wt.% TiO_2 in the pegmatites.

Results of REE phosphates U–Pb dating

The monazite-(Ce) crystals from the garnet-mica schists from Muráň were large enough (15–50 μm) to be analyzed by a standard LA-ICP-MS procedure. Their U and Th content reached 6000 and 42,000 ppm, respectively, the U/Th ratios being about 0.18 in average (Suppl. Table S5). The radiometric ages determined in the individual spots varied between 79 and 85 Ma, with a grand average of 83±0.5 Ma (Fig. 8).

Because of the minute size of the REE phosphate crystals in the samples from Bacúch, Jedľové Kostoľany, and Čierny Balog, a routine analysis with LA-ICP-MS was not possible. The ablated area was essentially always larger than the analyzed crystals themselves. For this reason, the ablated material included the host minerals, predominantly carbonates. For this purpose, several (up to 10) ablation spots were shot in the gangue minerals of thin sections. Doing so should estimate the magnitude and composition of the potential Pb contamination when at the ablation includes also the host minerals beyond the tiny REE phosphate crystals. The host minerals yield Pb intensities less than 40 cps and U–Th intensities less than 1 cps. Thus their influence is negligible. Sulfide minerals were not tested in order to avoid a Pb contamination of the laser cell and the mass spectrometer. The contamination from the sulfides was excluded by visual observation before start of the ablation because they would have been easily discerned in the reflected light installed in the laser cell.

The Th/U ratios were low, confirmed by both electron microprobe (Suppl. Table S4) and LA-ICP-MS analyses (Suppl. Table S6). Due to the high common Pb fraction, the Tera-Wasserburg lower intercept ages were calculated from the matrix-, drift- and fractionation corrected isotope ratios (Fig. 8).

In the samples from Čierny Balog, only xenotime-(Y) was found and analyzed. The measured ages show bimodal distribution (Fig. 9, Suppl. Fig. S2). The main peak is located at 85.5±2.8 Ma, a weaker peak is found at 148±12 Ma.

In the samples from Bacúch, both monazite-(Ce) and xenotime-(Y) were found during laser ablation. The measured ages vary from 87.3±2.1 to 91.6±5.0 Ma (Table 1, Suppl. Table S6, Fig. 8). No difference was found between the ages determined for monazite-(Ce) and those for xenotime-(Y).

In the samples from Jedľové Kostoľany, monazite-(Ce) and xenotime-(Y) were dated radiometrically. The age measured on monazite-(Ce) is 81.8±3.3 and that measured on xenotime-(Y) is 76.7±4.6 Ma (Fig. 8).

The samples from Čučma contained large xenotime-(Y) aggregates intergrown with apatite. Despite the large size of these aggregates, they possessed another challenge for the radiometric dating. The xenotime-(Y) crystals in these samples contain very high amount of uranium, such that reduction of the amount of ablated material was necessary. The spot size was 15 μm and frequency only 2 Hz.

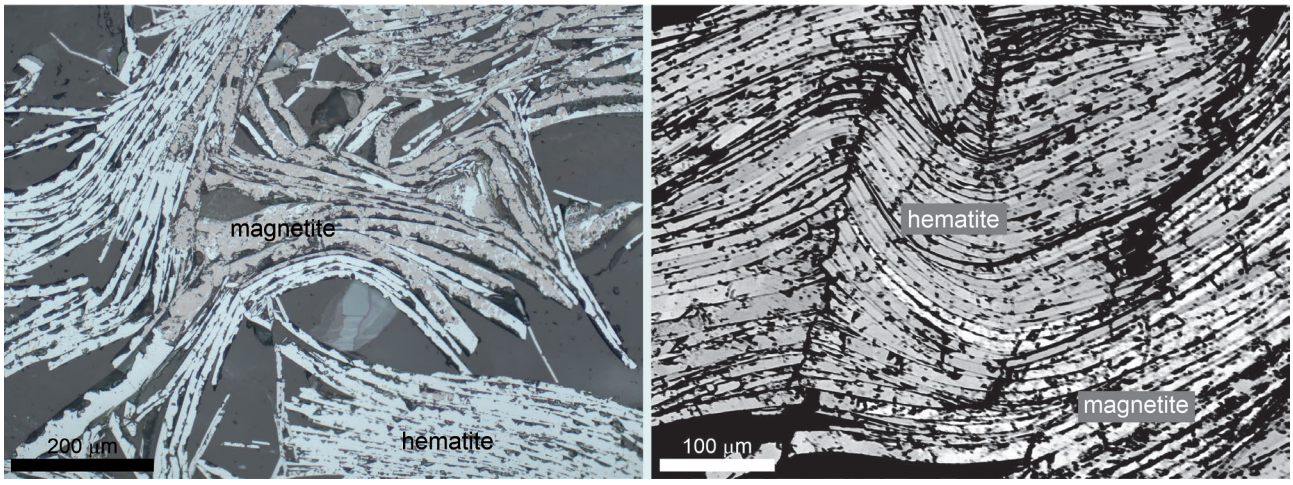

Fig. 7. Reflected-light image (left) and back-scattered electron image (right) of hematite from Magurka, with abundant mushketovitization (replacement of hematite by magnetite).

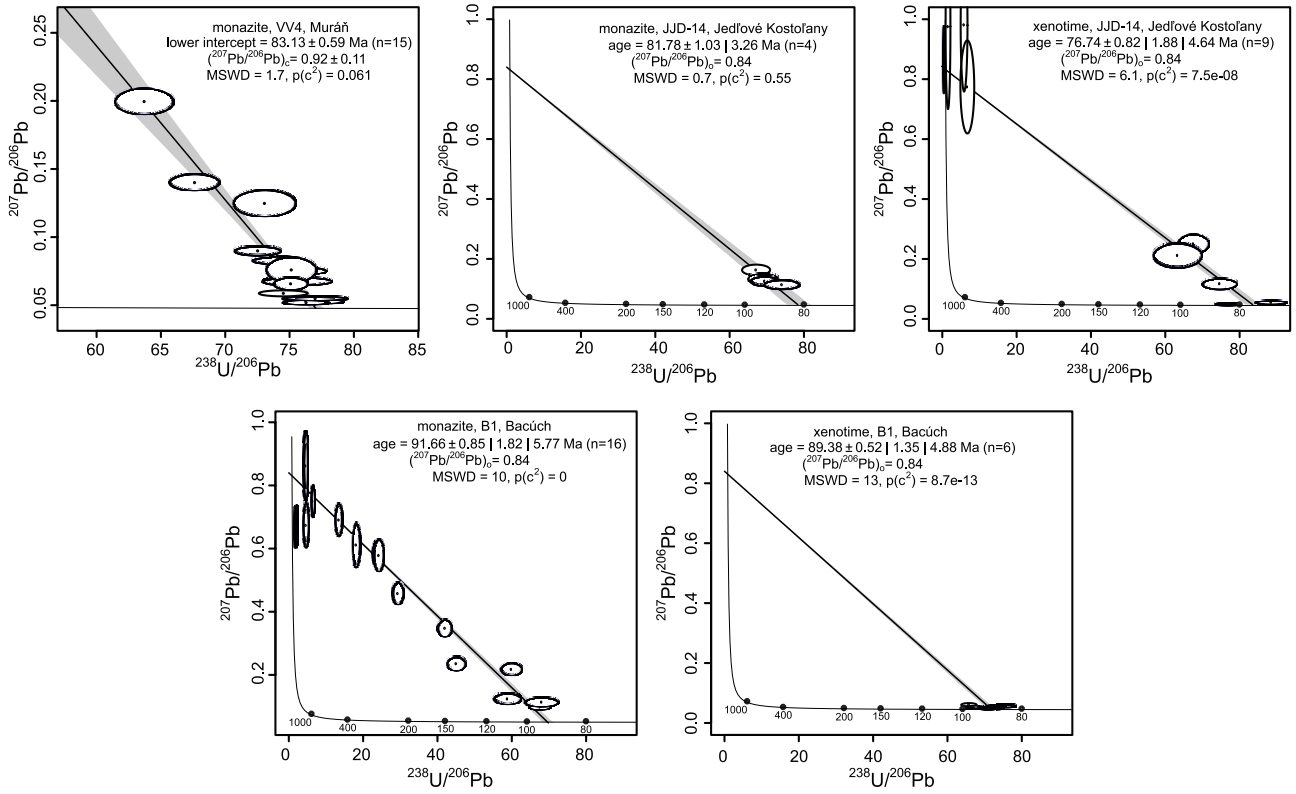

Fig. 8. Tera-Wasserburg diagrams for monazite-(Ce) and xenotime-(Y) from the studied localities. Mineral, sample ID, and the locality given in each panel. The reported mean ages correspond to the Stacey-Kramers anchored isochron ages.

The high U concentration raises suspicion that the xenotime-(Y) crystals contain submicroscopic inclusions of uraninite or a similar phase. The individual analyzed areas resulted in scattered ages. Neither the U content nor the Th/U ratio show any dependence on the ages. The pooled data includes 84 individual spots and the anchored lower intercept ages show a complex multimodal distribution (Fig. 9, Suppl. Fig. S2). Only the main age component of the distribution is well constrained and is located at 143±2 Ma, while the components isolated along the younger and older tails (ca. 106 Ma and 183±3 Ma) are more diffuse. The older age could be regarded as an asymmetrical tail of the distribution generated by mixing or by isotope exchange in an open system.

Results of hematite (U–Th)/He dating

The results of (U–Th)/He dating are presented in Table 2. Aliquots of sample MH-3 yielded relatively reproducible dates ranging from 95–100 Ma, with a weighted mean of 97.5±4.4 (2σ). In contrast, aliquots of sample MH-2 yielded dates ranging from 48–95 Ma, with a weighted mean of 71±40 (2σ). Neither sample shows inverse correlations between date and U concentration. With one exception of one aliquot with exceptionally high U, there is no difference between U or Th concentrations of the lased/degassed and unlased/undegassed aliquots. This is consistent with lack of U-volatilization during laser heating for He extraction (e.g., Hofmann et al. 2020), thus supporting the accuracy of the data.

Discussion

REE phosphates in the quartz–tourmaline stage in the Veporic unit – timing of the mineralization

Monazite-(Ce) and xenotime-(Y) are accessory minerals in the studied mineralizations. Among all hydrothermal minerals present, they are the most amenable ones to radiometric dating. They are, however, by no means restricted to the hydrothermal mineralizations but can be found also dispersed in the surrounding metamorphic rocks.

The oldest monazite in the metamorphic rocks of the Veporic Unit was found to be of Cenerian age (480–460 Ma), with Variscan (364±13 Ma) and Alpine (96±23 Ma) remobilization (Petrík et al. 2024). The breakdown of the primary, presumably Variscan monazite in the Veporic rocks was assigned to at least two events. The older one, of Permian age, is related to a Permian thermal event (Ondrejka et al. 2012, 2016). Permian monazites were also reported from andalusite-bearing micaschists near Pohorelá where ages of 278±5 Ma and 275±12 Ma date the HT-LP metamorphic assemblage (Jeřábek et al. 2008b). The younger event of monazite breakdown is of

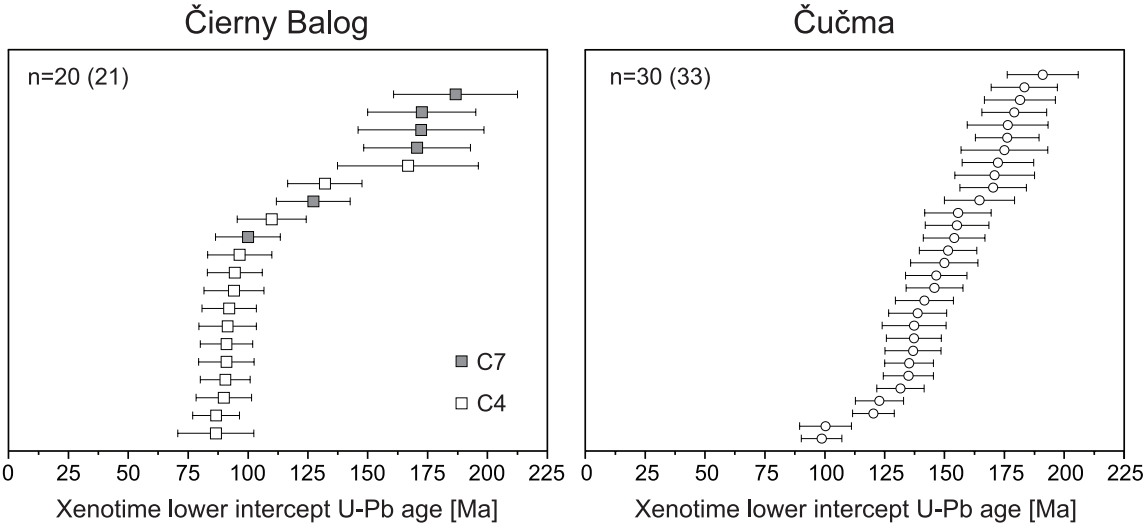

Fig. 9. Distribution of ages determined on xenotime-(Y) from the samples in Čierny Balog and Čučma.

Table 2: Results of the (U–Th)/He dating of the hematite samples from Magurka.

sample/aliquot	fmol He±2σ	μg U/g±2σ	μg Th/g±2σ	Th/U	date (Ma)±2σ	2σ (%)	weighted mean date ±2σ
MH-2/Fe1	163±1.5	4.99±0.14	2.87±0.083	0.589	47.5±1.3	2.7	71±40
MH-2/Fe2	214±2.0	2.12±0.06	2.23±0.065	1.08	95.4±2.4	2.5	
MH-2/Fe4	377±1.6	5.66±0.17	8.46±0.25	1.53	73.8±1.7	2.3	
MH-2/Fe5	89.1±0.6	2.68±0.08	2.32±0.067	0.886	53.2±1.3	2.5	
MH-2/Fe6	826±5.4	5.10±0.15	7.93±0.232	1.60	83.9±1.9	2.3	
MH-3/Fe1	586±5.7	5.49±0.16	2.60±0.076	0.485	94.9±2.6	2.7	97.5±4.4
MH-3/Fe2	813±2.9	5.65±0.16	1.16±0.034	0.210	97.8±2.6	2.7	
MH-3/Fe4	469±3.1	4.98±0.14	1.96±0.057	0.404	98.8±2.6	2.6	
MH-3/Fe5	338±0.7	5.58±0.16	1.32±0.039	0.243	95.5±2.5	2.6	
MH-3/Fe6	189±0.4	3.81±0.11	2.93±0.087	0.789	100.3±2.5	2.4	

Uncertainties are formal analytical precision taking into account uncertainty on He, U, Th measurements only.

Late Cretaceous age, related to metamorphism of the Veporic Unit. The metamorphic phengite there was dated to 100–85 Ma (Dallmeyer et al. 1996; Putiš et al. 2009b). The upper limit of this range is further confirmed by monazite in chloritoid–kyanite bearing Permian schists of the southern Veporic cover dated to 97±4 Ma (Bukovská et al. 2013). The lower end of this range, constrained also by zircon fission-track data (Plašienka et al. 2007; Vojtko et al. 2016), marks the onset of post-collisional exhumation. Continuing deformation was documented by slightly younger ages in strongly deformed igneous rocks in the vicinity of Bacúch (^{40}Ar–^{39}Ar ages of white mica of 78±1.3 Ma, Kohút et al. 2000).

Our samples from Muráň (samples VV4) reflect a substantial portion of this geological history. In our samples, the earlier garnet grains are assumed to be of Variscan age. The grossular-rich overgrowths were identified as Alpine garnets in numerous previous studies (e.g., Vrána 1980; Méres & Hovorka 1991; Kováčik 1996; Janák et al. 2001; Jeřábek et al. 2008a). The *P–T* conditions determined for the growth of Alpine garnets in similar samples of the same belt indicate prograde metamorphism reaching up to 620 °C at 9–10 kbar (Janák et al. 2001; Jeřábek et al. 2008a). This metamorphism is consistent with formation of the first deformation fabric in our samples. On the contrary, the secondary cleavage with fine grained muscovite–paragonite mixture is identical to the previously described subvertical cleavage for which lower *P–T* conditions of 450–550 °C at 5–8 kbar were estimated by Jeřábek et al. (2012). The development of this cleavage has been associated with exhumation of deep-seated rocks of the Veporic basement (Jeřábek et al. 2012; Vojtko et al. 2016). The age determined for the monazite-(Ce) crystals from our samples (83±0.5 Ma) coincides with the younger limit (85 Ma) of the range stated for the metamorphic phengite (Dallmeyer et al. 1996) as well as with Ar–Ar cooling ages reported from this belt (Maluski et al. 1993; Dallmeyer et al. 1996; Kováčik et al. 1996). All these data from the southern part of the Veporic unit coincide with the final stages of mid-Cretaceous thrusting and shortening of the northern part of the Veporic unit (Jeřábek et al. 2012; Plašienka 2018).

Around this time, the hydrothermal monazite-(Ce) and xenotime-(Y) crystals analyzed in this work were formed, as a result of deposition induced by falling temperature and pressure. Their chemical composition is distinct from that of the earlier REE phosphates. The Cretaceous REE phosphates are strongly depleted in Th and U (confirmed also by our LA-ICP-MS work) and enriched in Ca, Sr, and S (Pršek et al. 2010; Ondrejka et al. 2022). The conditions of their formation were estimated to 350–400 °C from CO_2-rich fluids (Ondrejka et al. 2022), these parameters being similar to those determined by fluid inclusions studies on the Alpine-type veins by Hurai et al. (1991).

Upon closer inspection, two groups of ages can be seen in our data (Table 1). There are older ages that cluster around 89 Ma from the locality Bacúch, comparable to the less precise ages reported from Ľubietová (Ozdín 2008). Both of these sites are located in the northern part of the Veporic unit. The ores at Bacúch are hosted by the metamorphosed autochthonous cover of the Veporic basement (so-called Jánov Grúň formation, Kotov et al. 1996). The ores at Ľubietová–Podlipa are hosted by the Permian metagraywackes (Vozárová & Vozár 1988; Jeřábek et al. 2012).

The youngest ages were recorded at Jedľové Kostoľany, corroborated by a similar age, albeit with lesser precision, reported by Ozdín (2008). This site is located in the northern part of the Tríbeč Mts, not in the main block of the Veporic unit. The affinity of the granitic rocks of the Tríbeč Mts to the Tatric or Veporic unit was disputed. Recently, Broska et al. (2024) showed that the southern part of the Tríbeč Mts is built by a tectonic duplex consisting of both types. The Tríbeč Mts experienced a protracted history of Alpine thrusting of granitic rocks over granitic rocks (Broska et al. 2024) which could be responsible for the younger ages detected also in this study. One sample of a differentiated granite dike in the S-type Tatric granite returned Alpine ages of monazite of 104±27 Ma. The K–Ar ages of muscovite of 75.3±0.4 to 81.9±1.7 Ma were interpreted as age that postdate the thrusting event.

Directly at the locality Jedľové Kostoľany, thin veinlets of hydrothermal muscovite (see Fig. 5) in carbonates were dated to 75.1±1 and 75.4±2 Ma (Ar–Ar ages, Chovan et al. 2006). Similar muscovite was found also in our samples along the boundaries of the siderite grains. The REE phosphates in Jedľové Kostoľany reflect the longer tectonic and hydrothermal history at this site compared to the sites located in the main Veporic block. The monazite-(Ce) age from this work essentially matches the Ar–Ar ages on muscovite, documenting hydrothermal activity at this time, preceding the formation of the sulfidic mineralization.

The new data confirm that the quartz–albite–chlorite veinlets with REE phosphates, tourmaline, and other minerals, either on their own or embedded in other types of mineralizations, can be directly linked to the post-peak metamorphic path in the Veporic Unit. This notion is also indirectly supported by the fact that monazite in the Tatric Unit (where there was no Alpine metamorphism) shows no Alpine breakdown and returns only Variscan ages (e.g., Uher et al. 2014).

REE phosphates in the quartz–tourmaline stage from the Gemeric unit – timing of the mineralization

The samples from Čučma (Gemeric unit) returned older ages that the samples of the REE phosphates from the Veporic unit investigated in this work. The main peak in the age distribution (Fig. 9), located at 143±2 Ma is close to the datum of 139±1 Ma determined by Hurai et al. (2015). They dated, by a similar method, monazite from albite metasomatic zone around a siderite–sulfide vein in Rožňava (Gemeric unit). These ages broadly agree with radiometric ages of siderite and ankerite from Dobšiná (Gemeric unit; Kiefer et al. 2020). Hence, the datum of ~140 Ma appears to be well constrained and was attached to the buildup of a deformation front in the Variscan basement in response to Early Cretaceous compression, folding, and thrusting (Hurai et al. 2015).

In the material from Čučma–Kutačka, used also in this work, Števko et al. (2014) performed chemical U–Pb dating of uraninite. The results ranged from 171 and 215±2 Ma, with a grand average of 207±2 Ma (Upper Triassic). They also reported younger ages (171 to 193±2 Ma) from minute (<10 μm) uraninite grains. The deviation toward younger ages in these grains was explained by episodic Pb loss during thermal overprinting or recrystallization (Števko et al. 2014). A weaker peak in our age distribution at 183±3 Ma could be seen as a support of such recrystallization event that preceded the major deformation phase in the Gemeric unit. A large spread of uraninite ages (determined by chemical U–Pb) dating was also reported by Demko et al. (2012). They investigated the U–Mo deposit Košice–Kurišková (Gemeric unit). Their ages lie in the range of 200–160 Ma and may coincide with local hydrothermal activity and remobilization during unroofing of the Variscan basement of the Gemeric unit and growth of the Meliata ocean basin (Putiš et al. 2012).

Constraints on the age of the siderite–ankerite and quartz–sulfide mineralization

In general, the "Alpine veins" with quartz, REE phosphates, adularia, and other minerals are placed between the siderite–ankerite and quartz–sulfide mineralization (Hurai et al. 2008; Majzlan et al. 2020a) in the Central Western Carpathians. This position constrains the age of the siderite–ankerite and quartz–sulfide mineralizations. The latter one was not dated so far, mainly because of absence of minerals amenable to dating.

The siderite–ankerite mineralization was dated only on samples from Dobšiná (Gemeric unit; Kiefer et al. 2020), giving scattered ages between 145±5 Ma to 114±24 Ma. These ages broadly overlap with the age range of metamorphism in the Gemeric unit. The age of 148±12 Ma, determined in the samples from Čierny Balog (Veporic unit) in this work (Fig. 9), could be tentatively assigned to the carbonates that host the analyzed xenotime-(Y). This time, however, distinctly predates the metamorphic peak in the Veporic unit (at ~110–100 Ma; Jeřábek et al. 2012). Interestingly, the ages of hydrothermal

dolomite that hosts tetrahedrite at the Dúbrava deposit (Tatric unit) range between 156±13 and 128±4 Ma (Majzlan et al. 2020b). At this time, the three units were still geographically separated and the match in the ages of the hydrothermal carbonates is perhaps only coincidental.

The quartz–sulfide mineralization is regionally distributed in the Gemeric, Veporic, and Tatric units. The upper boundary of 80–90 Ma for its age can be assumed from this work. This date is also confirmed by dating of the hydrothermal Ni–Co mineralization in Dobšiná to 93.6±0.9 Ma (Kiefer et al. 2020). The sulfides of the quartz–sulfide mineralization (chalcopyrite, tetrahedrite) heal fractures in the Ni–Co arsenides at this site. Plašienka et al. (2007) showed cooling of the Veporic–Gemeric contact zone to zircon fission-track closure temperature (240±50 °C) at 70–75 Ma (Late Cretaceous to earliest Paleogene), with a few outliers. According to these authors, the acquired ages generally match the exhumation trend of the Veporic metamorphic core complex. The southwestern part of the Veporic unit experienced the highest degree of Alpine metamorphism. Vojtko et al. (2017) documented cooling of the SW part of the Veporic unit to 320–200 °C at 61–55 Ma (Palaeocene) and down to 245–90 °C during 37–22 Ma (Eocene and Oligocene). These ages are the lowermost boundary for the quartz–sulfide mineralization whose formation temperature was estimated to 90–180 °C (Hurai et al. 2002). If taken at their face value, the quartz–sulfide mineralization could be even Tertiary, even though there are no other lines of support for this speculation at the moment. Late Cretaceous to Tertiary movement of warm hydrothermal fluids were documented from the Transdanubian range (Demény et al. 2024) and was likely sustained in large volumes of the activated Alpine crust throughout Tertiary.

Hematite–quartz stage – mineral assemblages, radiometric data, timing of the mineralization

Quartz–hematite veinlets are not restricted only to the vicinity of Magurka in the Nízke Tatry Mts. Similar veinlets were reported from other occurrences such as Jasenie–Soviansko (Luptáková 2007) and Trangoška (Láznička 1965). Luptáková (2007) reported quartz and hematite as two co-existing minerals, although she noted also the replacement of hematite by magnetite. She also studied fluid inclusions from quartz associated with hematite. They contained either aqueous phase and a gas bubble or an additional halite crystal at room temperature. The fluid inclusions showed a broad range of homogenization temperatures between 120–200 °C but a narrow range of salinities between 23–26 wt.% NaCl eq., with the ratio $CaCl_2/(CaCl_2+NaCl)$ varying between 0.27 and 0.78. Hematite veinlets of uncertain origin were also found in Považský Inovec Mts. hosted in Variscan quartz porphyries or Permian conglomerates (Hovorka 1960; Polák 1971).

Láznička (1965) described quartz, albite, chlorites, and weathered pyrite as minerals that accompany hematite. The mineralization is developed in Variscan granodiorites and high-grade metamorphic rocks on the southern slopes of the Nízke Tatry Mts. Koděra (1986, p. 483) assigned this mineralization to the "Alpine-veins", particularly common in the Veporic unit of the Western Carpathians. From the same region, Zoubek (1951) described hematite and quartz in veinlets in Alpine mylonite zones, located in porous sedimentary carbonates (so-called *rauhwacke*) and in sandstones.

For the quartz–hematite veinlets, with or without additional minerals, the geological, geochemical (fluid inclusion data), and geochronological evidence is compatible with the origin of the hydrothermal fluids for these mineralizations in overpressurized thrusting zones of the Alpine nappes. Such zones, if developed in sedimentary carbonate rocks, are recognized as so-called *rauhwacke*, or basal hydraulic breccias that facilitate the motion of the tabular block of the nappe (Milovský et al. 2012). According to this work, the fluids in the overpressurized, fluid-saturated sole of the moving nappe experienced temperatures of 400–450 °C and leached substantial amount of Si, Al, alkali metals, and phosphate from the surrounding rocks. They also stated that, upon opportunity, the fluids escaped this environment, circulated in the neighboring rocks and deposited their content at temperatures of 180–200 °C. In addition, the thrusting plane was commonly, but not always, located in rheologically weak rocks with evaporite components, thus enriching the fluids strongly in chloride and sulfate. All these fluid properties fit very well to those found in the studied mineralizations.

Hydrothermal vein carbonates near the quartz–hematite occurrences in the vicinity of Magurka described in this work were dated to 160–130 Ma (U–Pb, Majzlan et al. 2020b). The presented (U–Th)/He ages of hematite (Table 2) show large scatter for the sample MH-2 (71±40 Ma) but cluster much more tightly for the sample MH-3 (97.5±4.4 Ma). These ages, especially the tighter one, are compatible with the timing of thrusting of the Veporic unit northward first onto the Fatric Unit at ~110 Ma and later onto the Tatric unit at ~95 Ma (Plašienka 2003). The formation of hematite needs not be related to the major crustal fault separating the two units (the Čertovica fault) but could be linked to smaller subparallel thrusting planes. That would explain why the occurrences of quartz–hematite veinlets are scattered in several geographically disconnected localities in the Tatric basement and in the Lower-Triassic sandstones of the Nízke Tatry Mts.

The closure temperature for He diffusion in hematite varies strongly with particle size (Farley 2018). For large crystals, such as those in our study, it is as high as 250 °C. This temperature is somewhat higher than the formation temperature estimated from the fluid inclusion studies (Luptáková 2007). For this reason, the presented ages are not considered to be cooling, but rather the true formation ages.

Conclusions

This work addressed the question of timing of small hydrothermal mineralizations in Central Western Carpathians and the source of their fluids. The findings can be summarized in

a few paragraphs, noting that some of the working hypotheses were not confirmed.

The notion of the correlation of ages with the vergency of the Alpine orogen was verified to a certain extent. Monazite and xenotime at the site Čučma–Kutačka (dated to 143±2 Ma) in the Gemeric Unit originated at the boundary of Jurassic and Cretaceous. This mineralization broadly coincides with the metamorphic peak in the Gemeric Unit, formation of the Gemeric cleavage fan (CGF), and formation of hydrothermal siderite–ankerite veins in this region. An older, less pronounced peak in the age distribution (at 183±3 Ma) suggests that hydrothermal activity may have occurred also during unroofing of the Variscan basement of the Gemeric unit and growth of the Meliata ocean basin. Our results compare well with previous data from Rožňava and Košice–Kurišková.

The quartz–hematite mineralization in the Nízke Tatry Mts yielded different, older ages of around 97.5±4.4 Ma. The difference between the age of hematite in the Tatric Unit and that of monazite/xenotime in the adjacent part of Veporic Unit suggest that different processes were responsible for their formation.

The ages of monazite and xenotime in the Veporic and Tatric unit are significantly younger, varying between 77–92 Ma. There are age differences between the individual localities studied but these cannot be simply correlated to their current position within the orogen. Younger ages (77–86 Ma) were determined for samples from metamorphic rocks (Muráň) or the quartz–tourmaline stage (Čierny Balog, Jedľové Kostoľany) as opposed to samples from the metamorphosed Fe ores from Bacúch (87–92 Ma).

For the quartz–tourmaline stage ('Alpine veins') in the Veporic unit, the timing, position of the mineralization, and its mineralogical content suggest its linkage to the Alpine metamorphism in this unit. For the quartz–hematite mineralization in the Tatric unit, the more likely source of the fluids was the sole of the moving thick- or thin-skinned units thrusted over each other in Middle Cretaceous.

Acknowledgements: We dedicate this publication to Igor Broska, for his relentless friendship, enthusiasm, and excellent scientific insights in accessory minerals and granitic rocks of the Western Carpathians. We are thankful to Štefan Ferenc, Peter Koděra, and an anonymous reviewer for their constructive criticism, as well as to Milan Kohút and Martin Ondrejka for editorial handling and additional comments. We appreciate analytical assistance from Uttam Chowdhury. We thank Marian Janák for providing sample VV4 and Rober Holder for monazite analyses in this sample. This work was financially supported by a *Deutsche Forschungsgemeinschaft* grant MA 3927/43-1.

References

Aleinikoff J.N., Schenck W.S., Plank M.O., Srogi L.A., Fanning C.M., Kamo S.L. & Bosbyshell H. 2006: Deciphering igneous and metamorphic events in high-grade rocks of the Wilmington complex, Delaware: Morphology, cathodoluminescence and backscattered electron zoning, and SHRIMP U-Pb geochronology of zircon and monazite. *Geological Society of America Bulletin* 118, 39–64. https://doi.org/10.1130/B25659.1

Bezák V., Sassi F.P., Spišiak J. & Vozárová A. 1993: An outline of the metamorphic events recorded in the Western Carpathians (Slovakia). *Geologica Carpathica* 44, 351–364.

Broska I., Petrík I., Yi K., Majka J., Barnes C.J., Vojtko R., Madarás J., Kurylo S. & Kubiš M. 2024: Alpine stacking of two Variscan granite blocks recognised from mineral stabilities, age and structural data (Western Carpathians). *Chemical Geology* 648, 121959. https://doi.org/10.1016/j.chemgeo.2024.121959

Bukovská Z., Jeřábek P., Lexa O., Konopásek J., Janák M. & Košler J. 2013: Kinematically unrelated C-S fabrics: an example of extensional shear band cleavage from the Veporic Unit (Western Carpathians). *Geologica Carpathica* 64, 103–116. https://doi.org/10.2478/geoca-2013-0007

Cambel B., Jarkovský J., Faith L., Forgáč J., Hovorka D. & 21 authors 1985: Rudňany ore field. *Veda*, Bratislava, 1–363 (in Slovak).

Chovan M., Póč I., Jancsy P., Majzlan J. & Krištín J. 1995: Ore mineralization Sb–Au (As–Pb) at the Magurka deposit, Nízke Tatry Mts. *Mineralia Slovaca* 27, 397–406 (in Slovak).

Chovan M., Hurai V., Putiš M., Ozdín D., Pršek J., Moravanský D., Luptáková J., Zahradníková J., Kráľ J. & Konečný P. 2006: Fluid sources and formation of the mineralizations of the Tatric and northern Veporic units. *Open File Report, Comenius University*, Bratislava (in Slovak).

Dallmeyer R.D., Neubauer F., Handler R., Fritz H., Müller W., Pana D. & Putiš M. 1996: Tectonothermal evolution of the internal Alps and Carpathians: Evidence from $^{40}Ar/^{39}Ar$ mineral and whole-rock data. *Eclogae Geologicae Helvetiae* 89, 203–227.

Demény A., Rinyu L. & Dublyansky Y. 2024: Late Cretaceous to early Cenozoic hydrothermal fluid migration and red calcite formation in the Transdanubian Range, Hungary. *Geologica Carpathica* 75, 271–277. https://doi.org/10.31577/GeolCarp.2024.15

Demko R., Ferenc Š., Biroň A., Novotný L. & Bartalský B. 2012: The genesis of Kurišková U–Mo ore deposit. *Esemestník* 1, 24–25.

Dunkl I., Mikes T., Simon K. & von Eynatten H. 2008: Brief introduction to the Windows program Pepita: data visualization, and reduction, outlier rejection, calculation of trace element ratios and concentrations from LA-ICP-MS data. *Mineralogical Association of Canada, Short Course* 40, 334–340. https://doi.org/10.3749/9780921294801.app07

Evenson N.S., Reiners P.W., Spencer J.E. & Shuster D.L. 2014: Hematite and Mn oxide (U–Th)/He dates from the Buckskin–Rawhide detachment system, western Arizona: Gaining insights into hematite (U–Th)/He systematics. *American Journal of Science* 314, 1373–1435. https://doi.org/10.2475/10.2014.01

Farley K.A. 2018: Helium diffusion parameters of hematite from a single-diffusion-domain crystal. *Geochimica et Cosmochimica Acta* 231, 117–129. https://doi.org/10.1016/j.gca.2018.04.005

Faryad S.W. 1997: Metamorphic petrology of the Early Paleozoic low-grade rocks in the Gemericum. In: Grecula P., Hovorka D. & Putiš M. (eds.): Geological Evolution of the Western Carpathians. *Mineralia Slovaca, Geocomplex*, 309–314.

Faryad S.W., Ivan P. & Jedlička R. 2020: Pre-Alpine high-pressure metamorphism in the Gemer unit: mineral textures and their geodynamic implications for Variscan Orogeny in the Western Carpathians. *International Journal of Earth Sciences* 109, 1547–1564. https://doi.org/10.1007/s00531-020-01856-2

Friedl G., Quadt A.V. & Finger F. 1996: Timing der Intrusionstätigkeit im Südböhmischen Batholith. *TSK 6 Abstractband*, Facultas Universitätsverlag Wien, 127.

Garcia V.H., Reiners P.W., Shuster D.L., Idleman B. & Zeitler P.K. 2018: Thermochronology of sandstone-hosted secondary Fe- and Mn-oxides near Moab, Utah: Record of paleo-fluid flow along a fault. *GSA Bulletin* 130, 93–113. https://doi.org/10.1130/B31627.1

Grecula P., Abonyi A., Abonyiová M., Antaš J., Bartalský B., Bartalský J., Dianiška I., Drnzík E., Ďuďa R., Gargulák M., Gazdačko Ľ., Hudáček J., Kobulský J., Lörincz L., Macko J., Návesňák D., Németh Z., Novotný L., Radvanec M., Rojkovič I., Rozložník L., Rozložník O., Varček C. & Zlocha J. 1995: Mineral deposits of the Slovak Ore Mountains. *Mineralia Slovaca – Monograph*, 1–834.

Harrison M.T., Grove M., McKeegan K.D., Coath C.D., Lovera O.M. & Le Fort P. 1999: Origin and episodic emplacement of the Manaslu intrusive complex, Central Himalaya. *Journal of Petrology* 40, 3–19. https://doi.org/10.1093/petroj/40.1.3

Hofmann F., Treffkorn J. & Farley K.A. 2020: U-loss associated with laser-heating of hematite and goethite in vacuum during (U–Th)/He dating and prevention using high O_2 partial pressure. *Chemical Geology* 532, 119350. https://doi.org/10.1016/j.chemgeo.2019.119350

Horstwood M.S.A., Foster G.L., Parrish R.R., Noble S.R. & Nowell G.M. 2003: Common-Pb corrected in situ U–Pb accessory mineral geochronology by LA-MC-ICP-MS. *Journal of Analytical Atomic Spectrometry* 18, 837–846. https://doi.org/10.1039/B304365G

Hovorka D. 1960: Notes on quartz porphyres from the northern part of the Považský Inovec Mts. *Geologické Práce, Zprávy* 18, 65–70 (in Slovak).

Hurai V., Dávidová Š. & Kantor J. 1991: Adularia from alpine fissures of the Veporicum crystalline complexes: morphology, physical and chemical properties, fluid inclusion and K/Ar dating. *Mineralia Slovaca* 23, 133–144.

Hurai V., Simon K. & Bezák V. 1997: Contrasting chemistry and H, O, C isotope composition of greenschist-facies, Hercynian and Alpine metamorphic fluids (Western Carpathians). *Chemical Geology* 136, 281–293. https://doi.org/10.1016/S0009-2541(96)00135-0

Hurai V., Harčová E., Huraiová M., Ozdín D., Prochaska W. & Wiegerová V. 2002: Origin of siderite veins in the Western Carpathians I. *P–T–X*–δ^{13}C–δ^{18}O relations in ore-forming brines of the Rudňany deposits. *Ore Geology Reviews* 21, 67–101. https://doi.org/10.1016/S0169-1368(02)00082-3

Hurai V., Lexa O., Schulmann K., Montigny R., Prochaska W., Frank W., Konečný P., Kráľ J., Thomas R. & Chovan M. 2008: Mobilization of ore fluids during Alpine metamorphism: evidence from hydrothermal veins in the Variscan basement of Western Carpathians, Slovakia. *Geofluids* 8, 181–207. https://doi.org/10.1111/j.1468-8123.2008.00216.x

Hurai V., Paquette J-L., Lexa O., Konečný P. & Dianiška I. 2015: U–Pb–Th geochronology of monazite and zircon in albitite metasomatites of the Rožňava-Nadabula ore field (Western Carpathians, Slovakia): implications for the origin of hydrothermal polymetallic siderite veins. *Mineralogy and Petrology* 109, 519–530. https://doi.org/10.1007/s00710-015-0389-z

Jackson S.E., Pearson N.J., Griffin W.L. & Belousova E.A. 2004: The application of laser ablation-inductively coupled plasma-mass spectrometry to in situ U–Pb zircon geochronology. *Chemical Geology* 211, 47–69. https://doi.org/10.1016/j.chemgeo.2004.06.017

Janák M., Plašienka D., Frey M., Cosca M., Schmidt S.T., Lupták B. & Méres Š. 2001: Cretaceous evolution of a metamorphic core complex, the Veporic unit, Western Carpathians (Slovakia): P–T conditions and in situ Ar-40/Ar-39 UV laser probe dating of metapelites. *Journal of Metamorphic Geology* 19, 197–216. https://doi.org/10.1046/j.0263-4929.2000.00304.x

Janák M., Méres Š. & Medaris Jr. L.G. 2020: Eclogite facies meta-ultramafite from the Veporic Unit (Western Carpathians, Slovakia). *Geologica Carpathica* 71, 209–220. https://doi.org/10.31577/GeolCarp.71.3.1

Jeřábek P., Faryad W.S., Schulmann K., Lexa O. & Tajčmanová L. 2008a: Alpine burial and heterogeneous exhumation of Variscan crust in the West Carpathians: insight from thermodynamic and argon diffusion modelling. *Journal of the Geological Society* 165, 479–498. https://doi.org/10.1144/0016-76492006-165

Jeřábek P., Janák M., Faryad S.W., Finger F. & Konečný P. 2008b: Polymetamorphic evolution of pelitic schists and evidence for Permian low-pressure metamorphism in the Vepor Unit, West Carpathians. *Journal of Metamorphic Geology* 26, 465–485. https://doi.org/10.1111/j.1525-1314.2008.00771.x

Jeřábek P., Lexa O., Schulmann K. & Plašienka D. 2012: Inverse ductile thinning via lower crustal flow and fold-induced doming in the West Carpathian Eo-Alpine collisional wedge. *Tectonics* 31, TC5002. https://doi.org/10.1029/2012TC003097

Kiefer S., Števko M., Vojtko R., Ozdín D., Gerdes A., Creaser R.A., Szczerba M. & Majzlan J. 2020: Geochronological and geochemical constraints on the carbonate-sulfarsenide veins in Dobšiná, Slovakia: U/Pb ages of hydrothermal carbonates, Re/Os age of gersdorffite, and K/Ar ages of fuchsite. *Journal of Geosciences* 65, 229–247. https://doi.org/10.3190/jgeosci.314

Koděra M. (Ed.) 1986: Topographic Mineralogy of Slovakia. Volume 1. *Veda*, Bratislava (in Slovak).

Kohn M.J. & Vervoort J.D. 2008: U–Th–Pb dating of monazite by single-collector ICP-MS: Pitfalls and potential. *Geochemistry, Geophysics, Geosystems* 9, Q04031. https://doi.org/10.1029/2007GC001899

Kohút M. & Larionov A.N. 2021: From subduction to collision: Genesis of the Variscan granitic rocks from the Tatric Superunit (Western Carpathians, Slovakia). *Geologica Carpathica* 72, 96–113. https://doi.org/10.31577/GeolCarp.72.2.2

Kohút M., Frank W. & Petro M. 2000: The Sparistá dolina granitic mylonites – the products of the Alpine deformation. *Slovak Geological Magazine* 6, 347–361.

Kotov A.B., Miko O., Putiš M., Korikovsky S.P., Bereznaya N.G., Kráľ J. & Krist E. 1996: U/Pb dating of zircons of postorogenic acid metavolcanics and metasubvolcanics: A record of Permian–Triassic taphrogeny of the West-Carpathian basement. *Geologica Carpathica* 47, 73–79.

Kováčik M. 1996: Kyanite–magnesian chlorite schist and its petrogenetic significance (the Sinec massif, southern Veporic unit, Western Carpathians). *Geologica Carpathica* 47, 245–255.

Kováčik M., Kráľ, J. & Maluski H. 1996: Metamorphic rocks in the southern Veporicum basement: Their Alpine metamorphism and thermochronologic evolution. *Mineralia Slovaca* 28, 185–202.

Kylander-Clark A.R.C., Hacker B.R. & Cottle J.M. 2013: Laser-ablation split-stream ICP petrochronology. *Chemical Geology* 345, 99–112. https://doi.org/10.1016/j.chemgeo.2013.02.019

Láznička P. 1965: Mineralogical relations in central Slovakia. *Národní muzeum*, Praha, 1–35 (in Czech).

Lexa J., Bezák V., Elečko M., Mello J., Polák M., Potfaj M., Vozár J., Schnabll G.W., Pálenský P., Császár G., Ryłko W. & Mackiv B. 2000: Geological map of Western Carpathians and adjacent areas 1:500 000. *MŽP SR, ŠGÚDŠ*, Bratislava.

Lexa O., Schulmann K. & Ježek J. 2003: Cretaceous collision and indentation in the West Carpathians: View based on structural analysis and numerical modeling. *Tectonics* 22.6. https://doi.org/10.1029/2002TC001472

Ludwig K.R. 2012: User's manual for Isoplot 3.75: A geochronological Toolkit for Microsoft Excel. *Berkeley Geochronology Center Special Publication* 4, 1–70.

Luptáková J. 2007: Hydrothermal Pb–Zn mineralization in the Tatric tectonic unit of the Western Carpathians. *PhD Thesis, Comenius University*, Bratislava, 1–201 (in Slovak).

Luptáková J., Milovská S., Jeleň S., Mikuš T., Milovský R. & Biroň A. 2016: Primary ore Cu mineralization at the Ľubietová-Podlipa locality (Slovakia). *Acta Geologica Slovaca* 8, 175–194.

Majzlan J., Chovan M., Hurai V. & Luptáková J. 2020a: Hydrothermal mineralisation of the Tatric Superunit (Western Carpathians, Slovakia): I. A review of mineralogical, thermometry and isotope data. *Geologica Carpathica* 71, 85–112. https://doi.org/10.31577/GeolCarp.71.2.1

Majzlan J., Chovan M., Kiefer S., Gerdes A., Kohút M., Siman P., Konečný P., Števko M., Finger F., Waitzinger M., Biroň A., Luptáková J., Ackerman L. & Hora J.M. 2020b: Hydrothermal mineralisation of the Tatric Superunit (Western Carpathians, Slovakia): II. Geochronology and timing of mineralisations in the Nízke Tatry Mts. *Geologica Carpathica* 71, 113–133. https://doi.org/10.31577/GeolCarp.71.2.2

Maluski H., Rajlich P. & Matte P. 1993: ^{40}Ar–^{39}Ar dating of the Inner Carpathians Variscan basement and Alpine mylonitic overprinting. *Tectonophysics* 223, 313–337. https://doi.org/10.1016/0040-1951(93)90143-8

Méres Š. 2005: Major, trace element and REE geochemistry of metasedimentary rocks from the Malé Karpaty Mts. (Western Carpathians, Slovak Republic): Implications for sedimentary and metamorphic processes. *Slovak Geological Magazine* 11, 107–122.

Méres Š. & Hovorka D. 1991: Alpine metamorphic recrystallization of the pre-Carboniferous metapelites of the Kohút crystalline complex (the Western Carpathians). *Mineralia Slovaca* 23, 435–442.

Milovský R., van den Kerkhof A., Hoefs J., Hurai V. & Prochaska W. 2012: Cathodoluminescence, fluid inclusion and stable C–O isotope study of tectonic breccias from thrusting plane of a thin-skinned calcareous nappe. *International Journal of Earth Sciences* 101, 535–554. https://doi.org/10.1007/s00531-011-0685-8

Ondrejka M., Uher P., Putiš M., Broska I., Bačík P., Konečný P. & Schmiedt I. 2012: Two-stage breakdown of monazite by post-magmatic and metamorphic fluids: An example from the Veporic orthogneiss, Western Carpathians, Slovakia. *Lithos* 142–143, 245–255. https://doi.org/10.1016/j.lithos.2012.03.012

Ondrejka M., Putiš M., Uher P., Schmiedt I., Pukančík L. & Konečný P. 2016: Fluid-driven destabilization of REE-bearing accessory minerals in the granitic orthogneisses of North Veporic basement (Western Carpathians, Slovakia). *Mineralogy and Petrology* 110, 561–580. https://doi.org/10.1007/s00710-016-0432-8

Ondrejka M., Molnárová A., Putiš M., Bačík P., Uher P., Voleková B., Milovská S., Mikuš T. & Pukančík L. 2022: Hellandite-(Y)–hingganite-(Y)–fluorapatite retrograde coronae: a novel type of fluid-induced dissolution–reprecipitation breakdown of xenotime-(Y) in the metagranites of Fabova Hoľa, Western Carpathians, Slovakia. *Mineralogical Magazine* 86, 586–605. https://doi.org/10.1180/mgm.2022.7

Ozdín D. 2008: Mineralogy and genetical study of hydrothermal siderite-quartz-sulphidic veins in Jedľové Kostoľany, the Tribeč Mts. (Slovak Republic). *Mineralogia* 32, 122–123.

Ozdín D., Sejkora J. & Račko M. 2016: Dating and paragenetic description of hydrothermal mineralization near Ľubietová. In: Nerastné suroviny v 21. Storočí. *SNM,* Bratislava, 42–43 (in Slovak).

Petrík I., Janák M., Finger F., Kurylo S., Konečný P. & Vaculovič T. 2024: Ordovician (Cenerian) metamorphism in the Western Carpathians: Evidence from EMP monazite dating of polymetamorphosed granitoids in the Veporic unit, Slovakia. *Lithos* 476–477, 107600. https://doi.org/10.1016/j.lithos.2024.107600

Plašienka D. 2003: Development of basement-involved fold and thrust structures exemplified by the Tatric–Fatric–Veporic nappe system of the Western Carpathians (Slovakia). *Geodinamica Acta* 16, 21–38. https://doi.org/10.1016/S0985-3111(02)00003-7

Plašienka D. 2018: Continuity and episodicity in the early Alpine tectonic evolution of the Western Carpathians: How large-scale processes are expressed by the orogenic architecture and rock record data. *Tectonics* 37, 2029–2079. https://doi.org/10.1029/2017TC004779

Plašienka D., Broska I., Kissová D. & Dunkl I. 2007: Zircon fission-track dating of granites from the Vepor-Gemer Belt (Western Carpathians): constraints for the Early Alpine exhumation history. *Journal of Geosciences* 52, 113–123. https://doi.org/10.3190/jgeosci.009

Polák S. 1971: Contribution to the metallogenesis of the Považský Inovec Mts. *Mineralia Slovaca* 3, 237–242 (in Slovak).

Pršek J., Ondrejka M., Bačík P., Budzyń B. & Uher P. 2010: Metamorphic-hydrothermal REE minerals in the Bacúch magnetite deposit, Western Carpathians, Slovakia: (Sr,S)-rich monazite-(Ce) and Nd-dominant hingganite. *Canadian Mineralogist* 48, 81–94. https://doi.org/10.3749/canmin.48.1.81

Putiš M., Ivan P., Kohút M., Spišiak J., Siman P., Radvanec M., Uher P., Sergeev S., Larionov A., Méres Š., Demko R. & Ondrejka M. 2009a: Meta-igneous rocks of the West-Carpathian basement, Slovakia: indicators of Early Paleozoic extension and shortening events. *Bulletin de la Société géologique de France* 180, 461–471. https://doi.org/10.2113/gssgfbull.180.6.461

Putiš M., Frank W., Plašienka D., Siman P., Sulák M. & Biroň A. 2009b: Progradation of the Alpidic Central Western Carpathians orogenic wedge related to two subductions: constrained by $^{40}Ar/^{39}Ar$ ages of white micas. *Geodinamica Acta* 22, 31–56. https://doi.org/10.3166/ga.22.31-56

Putiš M., Kopp M., Snárska B., Koller F. & Uher P. 2012: The blueschist-associated perovskite–andradite-bearing serpentinized harzburgite from Dobšiná (the Meliata Unit), Slovakia. *Journal of Geosciences* 57, 221–240. https://doi.org/10.3190/jgeosci.128

Reiners P.W. 2005: Zircon (U–Th)/He thermochronometry. *Reviews in Mineralogy and Geochemistry* 58, 151–179. https://doi.org/10.2138/rmg.2005.58.6

Ring U. & Gerdes A. 2016: Kinematics of the Alpenrhein-Bodensee graben system in the Central Alps: Oligocene/Miocene transtension due to formation of the Western Alps arc. *Tectonics* 35, TC004085. https://doi.org/10.1002/2015TC004085

Sasvári T., Maťo Ľ. & Mihók J. 1996: Structural and mineralogical evaluation of the northern part of the Nižná Slaná ore field, the knowledges to indications on deep-seated continuation of siderite bodies of the exploitated deposits Ignác and Gampeľ. *Acta Montanistica Slovaca* 1, 261–280.

Schmid S.M., Bernoulli D., Fügenschuh B., Matenco L., Schefer S., Schuster R. et al. 2008: The Alpine–Carpathian–Dinaridic orogenic system: Correlation and evolution of tectonic units. *Swiss Journal of Geosciences* 101, 139–183. https://doi.org/10.1007/s00015-008-1247-3

Spišiak J., Kohút M., Butek J., Ferenc Š., Šimonová V., Kopáčik R. & Chew D. 2024: The petrology and geochronology of the gabbro–dioritoid rocks from Veľké Železné (Nízke Tatry Mts., Western Carpathians). *Geologica Carpathica* 75, 3–20. https://doi.org/10.31577/GeolCarp.2024.02

Stacey J.S. & Kramers J. 1975: Approximation of terrestrial lead isotope evolution by a two-stage model. *Earth and Planetary Science Letters* 26, 207–221. https://doi.org/10.1016/0012-821X(75)90088-6

Števko M., Uher P., Ondrejka M., Ozdín D. & Bačík P. 2014: Quartz–apatite–REE phosphates–uraninite vein mineralization near Čučma (eastern Slovakia): a product of early Alpine hydrother-

mal activity in the Gemeric Superunit, Western Carpathians. *Journal of Geosciences* 59, 209–222. https://doi.org/10.3190/jgeosci.169

Vermeesch P. 2018: IsoplotR: a free and open toolbox for geochronology. *Geoscience Frontiers* 9, 1479–1493. https://doi.org/10.1016/j.gsf.2018.04.001

Vojtko R., Králiková S., Jeřábek P., Schuster R., Danišík M., Fügenschuh B., Minár J. & Madarás J. 2016: Geochronological evidence for the Alpine tectono-thermal evolution of the Veporic Unit (Western Carpathians, Slovakia). *Tectonophysics* 666, 48–65. https://doi.org/10.1016/j.tecto.2015.10.014

Vojtko R., Králiková S., Andriessen P., Prokešová R., Minár J. & Jeřábek P. 2017: Geological evolution of the southwestern part of the Veporic Unit (Western Carpathians): based on fission track and morphotectonic data. *Geologica Carpathica* 68, 285–302. https://doi.org/10.1515/geoca-2017-0020

Vozárová A. & Vozár J. 1988: Late Paleozoic in the Western Carpathians. *GÚDŠ*, Bratislava, 1–314.

Vrána S. 1980: Newly-formed Alpine garnets in metagranitoids of the Veporides in relation to the structure of the Central zone of the West Carpathians. *Časopis pro Mineralogii a Geologii* 25, 41–54.

Uher P., Kohút M., Ondrejka M., Konečný P. & Siman P. 2014: Monazite-(Ce) in Hercynian granites and pegmatites of the Bratislava Massif, Western Carpathians: compositional variations and Th–U–Pb electron-microprobe dating. *Acta Geologica Slovaca* 6, 215–231.

Zoubek V. 1951: Report of geological research on the southern slope of Nízke Tatry Mts between Bystrá and Jasenská valley. *Věstník Ústředního Ústavu geologického* 26, 162–166 (in Czech).

Electronic supplementary material is available online:
Suppl. Table S1 at https://geologicacarpathica.com/data/files/supplements/GC-76-Majzlan_TableS1.docx
Suppl. Tables S2 and S3 at https://geologicacarpathica.com/data/files/supplements/GC-76-Majzlan_TablesS2-S3.xlsx
Suppl. Tables S4 and S5 at https://geologicacarpathica.com/data/files/supplements/GC-76-Majzlan_TablesS4-S5.xlsx
Suppl. Table S6 at https://geologicacarpathica.com/data/files/supplements/GC-76-Majzlan_TableS6.xlsx
Suppl. Figs. S1 and S2 at https://geologicacarpathica.com/data/files/supplements/GC-76-Majzlan_FigsS1-S2.docx